Tonkie Khimicheskie Tekhnologii = Fine Chemical Technologies.
2026;21(1):109–119 ISSN 2686-7575 (Online)

Chemistry and technology of inorganic materials
Химия и технология неорганических материалов

UDC 544.032.3; 544.032.3; 544.034.2; 544.034.7; 544.431.22
https://doi.org/10.32362/2410-6593-2026-21-1-109-119
EDN PBLSBF

RESEARCH ARTICLE

Surface and bulk thermodynamic factors of $Ba_{0.5}Sr_{0.5}(Co_{0.8}Fe_{0.2})_{1-x}Me_xO_{3-\delta}$ (Me = Ta, W) oxides

Albert R. Akhmadeev[1],✉, Vadim A. Eremin[1], Maxim V. Ananyev[1,2]

[1] *Federal State Research and Design Institute of Rare Metal Industry (Giredmet), Moscow, 111524 Russia*
[2] *Mendeleev University of Chemical Technology of Russia, Moscow, 125047 Russia*
✉ *Corresponding author, e-mail: albertakhmadeev1@gmail.com*

Abstract

Objectives. In this work, we consider the relationship between the tracer (k^*) and chemical (k^δ) oxygen exchange coefficients for $Ba_{0.5}Sr_{0.5}(Co_{0.8}Fe_{0.2})_{1-x}Me_xO_{3-\delta}$ (Me = Ta, W) oxides. The aim is to analyze the experimental dependencies of the chemical (k^δ) and tracer (k^*) coefficients of oxygen exchange, evaluate the surface thermodynamic factor $w_0\big|_{x=\pm L}$, and compare its value with the bulk thermodynamic factor $w_0\big|_{x=0}$ determined from the dependence of oxygen content in oxides on the temperature and partial pressure of oxygen. Possible reasons for the discrepancy between these two thermodynamic factors are discussed.

Methods. The oxygen exchange kinetics between the gas phase and the surface of oxide materials under nonequilibrium conditions was studied using the method of oxygen pressure relaxation. The surface thermodynamic factor was calculated based on data obtained under both equilibrium and nonequilibrium conditions.

Results. Comparison of the tracer (k^*) and chemical (k^δ) oxygen exchange coefficients allowed the $w_0\big|_{x=\pm L}$ surface thermodynamic factor to be estimated by the $k^\delta = k^* w_0\big|_{x=\pm L}$ equation.

Conclusions. The surface thermodynamic factor was found to differ from the bulk thermodynamic factor of the oxide material, $w_0 = \frac{1}{2}\frac{\partial \ln\left(p_{O_2}\right)}{\partial \ln(3-\delta)}$, which can be calculated from the dependence of oxygen content in oxides on the temperature and partial pressure of oxygen. This difference can be explained by the difference in the defect structure of the surface layers of oxide materials.

Keywords

surface oxygen exchange, oxygen diffusion, BSCF, oxygen pressure relaxation, mixed ionic-electronic conduction membrane, thermodynamic factor

Submitted: 08.10.2024
Revised: 19.09.2025
Accepted: 19.01.2026

For citation

Akhmadeev A.R., Eremin V.A., Ananyev M.V. Surface and bulk thermodynamic factors of $Ba_{0.5}Sr_{0.5}(Co_{0.8}Fe_{0.2})_{1-x}Me_xO_{3-\delta}$ (Me = Ta, W) oxides. *Tonk. Khim. Tekhnol. = Fine Chem. Technol.* 2026;21(1):109–119. https://doi.org/10.32362/2410-6593-2026-21-1-109-119

НАУЧНАЯ СТАТЬЯ

Объемный и поверхностный термодинамические факторы оксидов $Ba_{0.5}Sr_{0.5}(Co_{0.8}Fe_{0.2})_{1-x}Me_xO_{3-\delta}$ (Me = Ta, W)

А.Р. Ахмадеев[1,✉], В.А. Еремин[1], М.В. Ананьев[1, 2]

[1] *Государственный научно-исследовательский и проектный институт редкометаллической промышленности (АО «Гиредмет»), Москва, 111524 Россия*

[2] *Российский химико-технологический университет им. Д.И. Менделеева, Москва, 125047 Россия*

✉ *Автор для переписки, e-mail: albertakhmadeev1@gmail.com*

Аннотация

Цели. Работа посвящена анализу взаимосвязи изотопного k^* и химического k^δ коэффициентов обмена кислородом для оксидов $Ba_{0.5}Sr_{0.5}(Co_{0.8}Fe_{0.2})_{1-x}Me_xO_{3-\delta}$ (Me = Ta, W). Целью работы является анализ экспериментальных зависимостей химического и изотопного коэффициентов обмена кислорода, оценка поверхностного термодинамического фактора $w_0\big|_{x=\pm L}$ и сравнение его с объемным термодинамическим фактором $w_0\big|_{x=0}$, определенным из зависимости содержания кислорода в оксидах от температуры и парциального давления кислорода. В статье обсуждаются возможные причины несовпадения двух термодинамических факторов.

Методы. Изучение кинетики обмена кислородом газовой фазы с поверхностью оксидных материалов в неравновесных условиях проведено методом релаксации давления кислорода. Расчет поверхностного термодинамического фактора проведен на основе данных, полученных в равновесных и неравновесных условиях.

Результаты. Сравнение изотопного k^* и химического k^δ коэффициентов обмена кислорода позволило оценить поверхностный термодинамический фактор $w_0\big|_{x=\pm L}$ через уравнение $k^\delta = k^* w_0\big|_{x=\pm L}$.

Выводы. Было обнаружено, что поверхностный термодинамический фактор отличается от термодинамического фактора, относящегося к объему оксидного материала $w_0 = \frac{1}{2}\frac{\partial \ln\left(p_{O_2}\right)}{\partial \ln\left(3-\delta\right)}$, который может быть рассчитан из зависимостей содержания кислорода в оксидах от температуры и парциального давления кислорода. Такое различие было объяснено различием в дефектной структуре поверхностных слоев оксидных материалов.

Ключевые слова

поверхностный обмен кислорода, диффузия кислорода, BSCF, релаксация давления кислорода, мембрана со смешанной ионно-электронной проводимостью, термодинамический фактор

Поступила: 08.10.2024
Доработана: 19.09.2025
Принята в печать: 19.01.2026

Для цитирования

Ахмадеев А.Р., Еремин В.А., Ананьев М.В. Объемный и поверхностный термодинамические факторы оксидов $Ba_{0.5}Sr_{0.5}(Co_{0.8}Fe_{0.2})_{1-x}Me_xO_{3-\delta}$ (Me = Ta, W). *Тонкие химические технологии*. 2026;21(1):109–119. https://doi.org/10.32362/2410-6593-2026-21-1-109-119

INTRODUCTION

Mixed oxygen-electronic conduction (MOEC) oxides have found wide application in high-temperature electrochemical devices, such as solid oxide fuel cells and electrolyzers, membranes for selective oxygen separation, and catalytic membrane reactors [1–3]. Oxygen transport membrane (OTM) technology, the most promising application of MOEC oxides, is considered an accessible and affordable method for producing high-purity (over 99%) oxygen [4, 5], as well as a basis for partial and selective catalytic oxidation of hydrocarbons [6, 7]. The main challenge in developing such membranes is to identify a suitable oxide material that could meet the requirements of mechanical strength, chemical resistance, and high oxygen flux through the membrane.

The oxygen flux is influenced by both the mobility of oxygen ions within the OTM and the rate of oxygen reduction/oxidation reactions on both sides of the membrane [8–13]. At a given temperature T and partial pressure of oxygen p_{O_2}, the oxygen flux through the membrane can be limited either by a surface reaction or by oxygen diffusion, which depends on the membrane thickness. In order to separate the contribution of each process to the total oxygen flux, Bouwmeester *et al*. [8] derived an expression for calculating the characteristic thickness L_c, which is defined as $L_c = \frac{D_0}{k_s}$, wherein D_0 is the oxygen self-diffusion coefficient, and k_s is the surface oxygen exchange coefficient. It should be noted that this formula for L_c is valid for oxides with predominantly electronic conduction. Under given experimental conditions (T and p_{O_2}), the total oxygen flux through a membrane with a thickness exceeding L_c is determined by the rate of oxygen diffusion in the bulk. In this case, the oxygen flux through the membrane is proportional to the ambipolar electrical conductivity σ_{amb} in accordance with Wagner's approach [14–16] and is expressed by the formula

$$J_{O_2} = -\frac{RT}{16F^2L}\int_{\ln(p'_{O_2})}^{\ln(p''_{O_2})}\sigma_{amb}\,d\ln\left(p_{O_2}\right), \quad (1)$$

$$\sigma_{amb} = \frac{\sigma_{ion}\sigma_{el}}{\sigma_{ion}+\sigma_{el}}, \quad (2)$$

wherein R is the universal gas constant; T is the absolute temperature; F is the Faraday constant; L is the membrane thickness; p_{O_2} is the partial pressure of oxygen; σ_{ion} is the oxygen-ionic conductivity; σ_{el} is the electronic conductivity; and p'_{O_2} and p''_{O_2} are the partial pressures of oxygen on the one and other sides of the membrane, respectively.

For oxides with predominantly electronic conductivity, oxygen ion diffusion is the limiting factor in membrane performance. Conversely, for membranes thinner than L_c, the oxygen flux is primarily determined by oxygen exchange reactions on the surface. At a sufficiently low gradient of the oxygen chemical potential on the surface, the reaction rate is proportional to the difference between the oxygen concentration on the surface at a given time and the equilibrium oxygen concentration, and the oxygen exchange rate constant is the proportionality constant. Consequently, both kinetic parameters—the oxygen diffusion coefficient D_0 and the surface exchange coefficient k_s—can serve as criteria for selecting an oxide material for OTMs (Fig. 1).

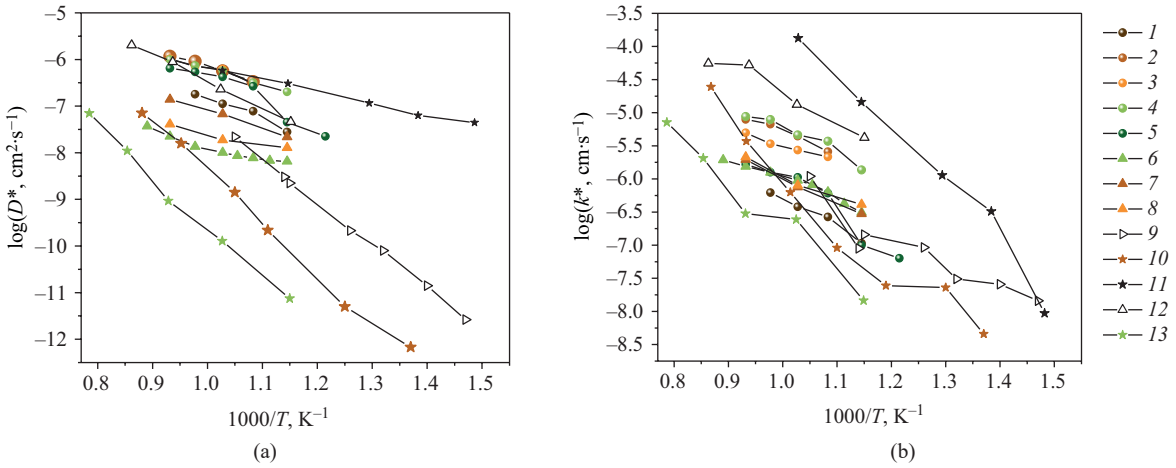

Fig. 1. Temperature dependencies of the (a) tracer oxygen diffusion coefficient D^* and (b) tracer oxygen exchange coefficient k^* of MOEC oxides. Lines are shown for perception convenience: (*1*) $Ba_{0.5}Sr_{0.5}Co_{0.725}Fe_{0.125}Ta_{0.15}O_{3-\delta}$ [17], (*2*) $Ba_{0.5}Sr_{0.5}Co_{0.78}Fe_{0.2}W_{0.02}O_{3-\delta}$ [17], (*3*) $Ba_{0.5}Sr_{0.5}Co_{0.775}Fe_{0.175}Nb_{0.05}O_{3-\delta}$ [17], (*4*) $Ba_{0.5}Sr_{0.5}Co_{0.775}Fe_{0.175}Nb_{0.05}O_{3-\delta}$ [17], (*5*) $Ba_{0.5}Sr_{0.5}Co_{0.8}Fe_{0.2}O_{3-\delta}$ [18], (*6*) $GdBaCo_2O_{6-\delta}$ [19], (*7*) $PrBaCo_2O_{6-\delta}$ [19], (*8*) $SmBaCo_2O_{6-\delta}$ [19], (*9*) $La_{0.6}Sr_{0.4}CoO_{3-\delta}$ [20], (*10*) $La_{0.6}Sr_{0.4}Co_{0.8}Fe_{0.2}O_{3-\delta}$ [21], (*11*) $Ba_{0.5}Sr_{0.5}Co_{0.8}Fe_{0.2}O_{3-\delta}$ [22], (*12*) $Sm_{0.5}Sr_{0.5}CoO_{3-\delta}$ [23], (*13*) $La_{0.8}Sr_{0.2}CoO_{3-\delta}$ [24]

It can be seen from Fig. 1 that the $Ba_{0.5}Sr_{0.5}Co_{0.8}Fe_{0.2-}O_{3-\delta}$ barium strontium cobaltite ferrite (BSCF) oxide exhibits the highest values of surface oxygen exchange and oxygen diffusion coefficients among oxides of various compositions. Indeed, BSCF oxides have attracted attention due to their exceptional oxygen ion transport rate at elevated temperatures. BSCF oxides possess a large number of mobile oxygen vacancies [18, 22, 25–32] in their highly symmetric perovskite lattice, which ensures a high oxygen flux over a wide temperature range.

Currently, the oxygen diffusion coefficient D_0 and the surface exchange coefficient k_s can be estimated using two fundamentally different experimental techniques, including tracer oxygen exchange and relaxation methods. Tracer oxygen exchange methods can be carried out under adsorption–desorption equilibrium conditions. In this case, the ^{18}O tracer concentration gradient between the gas phase and the solid phase acts as a driving force behind the gas-phase composition equilibration process, while the ambient oxygen pressure and, consequently, oxygen content in the oxide material remain constant.

The fundamental condition of adsorption–desorption equilibrium, which is inherent in tracer methods, is not met when using relaxation methods. This leads to a difference in oxygen content between the gas phase and the bulk of the oxide material. During sample equilibration with the environment, the oxygen content in the bulk of the oxide material, as well as parameters related to its content in the sample (mass, electrical conductivity, or oxygen pressure around the oxide), changes to a value corresponding to the equilibrium state. The chemical oxygen diffusion coefficient D_0^δ and the chemical oxygen exchange coefficient k^δ, which are found by relaxation methods, are related to the tracer oxygen diffusion coefficient D_0^* and the tracer oxygen exchange coefficient k^*, which are determined by tracer oxygen exchange methods, through the thermodynamic factor w_0 [33] under the condition that the oxide be predominantly an electronic conductor and the correlation effect be negligible:

$$k^\delta = k^* w_0\big|_{x=\pm L}, \quad (3)$$

$$D_0^\delta = D_0^* w_0\big|_{x=0}, \quad (4)$$

wherein

$$w_0 = \frac{1}{2}\frac{\partial \ln\left(p_{O_2}\right)}{\partial \ln\left(3-\delta\right)}. \quad (5)$$

The thermodynamic factor reflects the oxygen capacity of the oxide system and is related to the concentration of oxygen vacancies; therefore, it characterizes the response of the oxide system to changes in the partial pressure of oxygen. From general considerations, the bulk thermodynamic factor $w_0\big|_{x=0}$ and the surface thermodynamic factor $w_0\big|_{x=\pm L}$ are expected to have different values. This is related to the different structure of defects in the bulk and on the surface, which has been observed for various oxide materials [17, 19, 23, 34–36]. While the bulk thermodynamic factor $w_0\big|_{x=0}$ can be estimated directly from the dependence of oxygen content in the oxide on the partial pressure of oxygen, the same approach is difficult to apply to the surface thermodynamic factor $w_0\big|_{x=\pm L}$. Instead, the latter can be calculated directly using Eq. (3) provided that both kinetic constants are known.

In this work, we aim to analyze experimental dependencies of the chemical (k_δ) and tracer (k^*) oxygen exchange coefficients, estimate the surface thermodynamic factor $w_0\big|_{x=\pm L}$, and compare its value with the bulk thermodynamic factor $w_0\big|_{x=0}$ determined from the dependencies of oxygen content in oxides on temperature and partial pressure of oxygen. Further, we discuss possible reasons for the discrepancy between these two thermodynamic factors.

EXPERIMENTAL

Samples

The research objects in this work were $Ba_{0.5}Sr_{0.5}Co_{0.8}Fe_{0.2-}O_{3-\delta}$ (BSCF), $Ba_{0.5}Sr_{0.5}Co_{0.725}Fe_{0.125}Ta_{0.15-}O_{3-\delta}$ (BSCFTa15), and $Ba_{0.5}Sr_{0.5}Co_{0.78}Fe_{0.2}W_{0.02}O_{3-\delta}$ (BSCFW2) oxides. All oxides were synthesized by the solid-phase method [37]. $BaCO_3$, $SrCO_3$, Co_3O_4, Fe_2O_3, W, and Ta with a purity of at least 99.9% (*RusKhim*, Russia) were used as initial reagents. The synthesized samples were then pressed into cylindrical tablets followed by annealing in air at 1300°C for 7 h.

All the studied oxides were characterized in detail in our previous work [17]. The crystal structure of the synthesized oxides was examined using a Rigaku D/MAX-2200VL/PC diffractometer (*Rigaku*, Japan). According to X-ray powder diffraction analysis, the samples were single-phase and exhibited a cubic structure (space group $Pm\bar{3}m$). The surface morphology and elemental composition were investigated by scanning electron microscopy using a MIRA 3 LMU microscope (*TESCAN*, Czech Republic). Analysis of backscattered electron images revealed that all oxides were homogeneous in the bulk and had no additional phases different in terms of chemical composition.

Oxygen pressure relaxation

The kinetics of oxygen exchange was studied using the method of oxygen pressure relaxation. This method

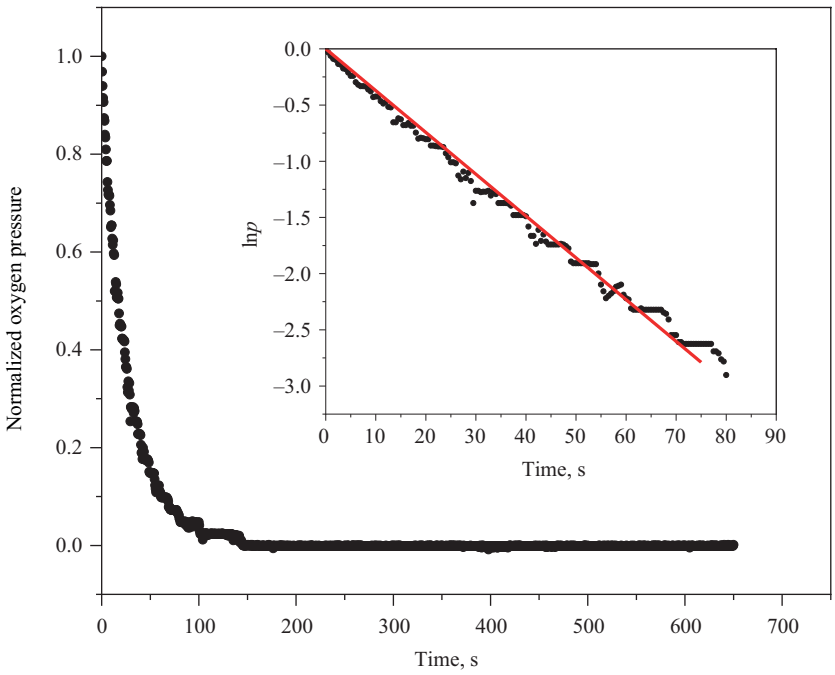

Fig. 2. Time dependence of normalized oxygen pressure p during equilibration from 1.33 to 3.06 mbar at 750°C. The inset shows the same dependence in semilogarithmic coordinates [38]

consists in a stepwise change in oxygen pressure above an oxide sample in a closed space of known volume, followed by recording the relaxation curve of oxygen pressure. Figure 2 presents a typical oxygen pressure relaxation curve corresponding to a step from 1.33 to 3.06 mbar at a temperature of 750°C. The experimental setup and experimental conditions were described in detail earlier [38].

Similar relaxation curves were obtained for other oxygen pressure jumps over the temperature range of 600–800°C and at oxygen pressures of 1–35 mbar. The equilibration process was carried out in both oxidation and reduction directions at a temperature of 700°C and a final pressure of 7 mbar. No statistically significant differences were found in the recorded oxidation and reduction relaxation curves.

In the corresponding coordinates, the time dependence of the natural logarithm of the normalized oxygen pressure p is linear (Fig. 2, inset), and any deviation from linearity is due to slow oxygen diffusion in the bulk of the oxide. Using the data obtained from the tracer oxygen exchange experiment in previous studies [17, 18], the characteristic thicknesses of the BSCF, BSCFTa15, and BSCFW2 oxides can be calculated to be 0.4, 0.3, and 0.16 cm, respectively (at 700°C and 6.5 mbar). Since the thicknesses of the oxide samples in this study did not exceed the corresponding characteristic thicknesses (less than 0.08 cm), it can be assumed that oxygen exchange during equilibration is governed primarily by the surface oxygen exchange reaction. This assumption is confirmed by the linearity of the time dependence of the normalized oxygen pressure in semilogarithmic coordinates (Fig. 2). From the obtained linear time dependencies, the chemical oxygen exchange coefficient k^{δ} can be calculated.

RESULTS AND DISCUSSION

The calculated values of the chemical oxygen exchange coefficients k^{δ}, as well as their temperature and pressure dependencies, are available in the literature [38] (Fig. 3). It was shown that the absolute values of chemical oxygen exchange coefficients k^{δ}, as well as exponents n in the pressure dependencies $k^{\delta} \sim p_{O_2}^{n}$ for the BSCF and BSCFTa15 oxides ($n \approx 0.5$), differ from those for BSCFW2 ($n \approx 0.25$).

The observed differences between the values of exponents n of pressure dependencies for the BSCF and BSCFTa15 oxides ($n \approx 0.5$) and the BSCFW2 oxide ($n \approx 0.25$) were explained within the framework of Fleig's *et al*. theory [39]. During pressure relaxation at the onset of oxygen exchange, the degree of surface coverage by the dominant type of ionized oxygen species changes; therefore, it is assumed that the rate of oxygen exchange during oxygen pressure equalization is directly proportional to the degree of surface coverage by ionized oxygen species. In this case, the dependence of oxygen exchange rate r^{δ} during oxygen pressure equalization on p_{O_2} will be directly proportional to the dependence $[\theta_j] = f(p_{O_2})$ of the degree $[\theta_j]$ of surface coverage

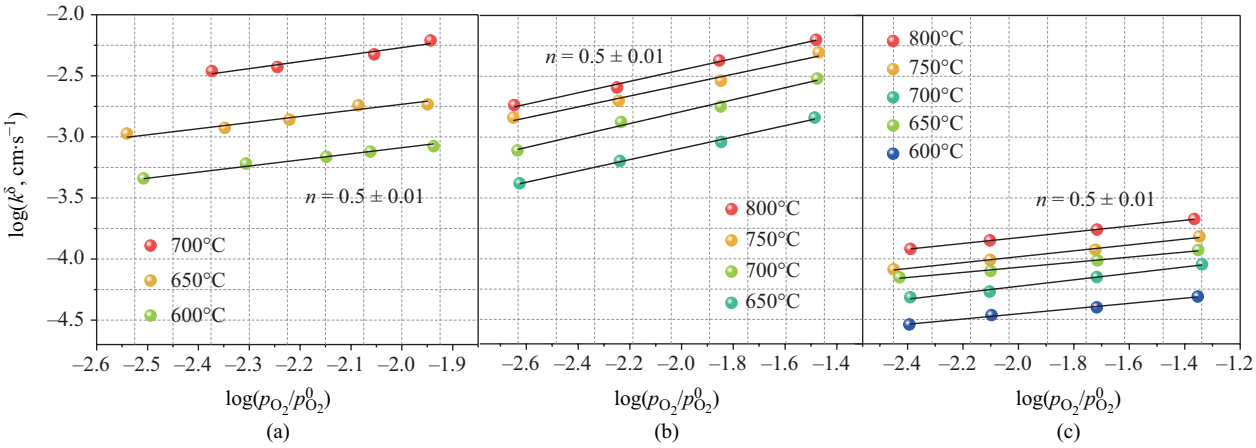

Fig. 3. Dependencies of chemical oxygen surface exchange coefficient k^δ on oxygen pressure: (a) BSCF, (b) BSCFTa15, and (c) BSCFW2 [38]

by ionized oxygen species O^-_{ad}, $O^-_{2,ad}$, or $O^{2-}_{2,ad}$ on p_{O_2}; j is the type of particles that cover the surface. Then,

$$r^\delta \propto [\theta_j]. \quad (6)$$

The oxygen exchange rate r^δ is related to k^δ via the formula

$$k^\delta = r^\delta \frac{M_r}{n_O^{ox} N_A \rho}, \quad (7)$$

wherein M_r is the molar mass of the oxide; n_O^{ox} is the oxygen content in the oxide, including the oxygen species on the surface; N_A is the Avogadro constant; and ρ is the crystallographic density.

The exponent of the dependence of k^δ on oxygen pressure thus correlates with the exponent of the dependence of $[\theta_j]$ on oxygen pressure. Thus, at the exponent $n \approx 0.5$ for the BSCF and BSCFTa15 oxides, the dominant species were shown to be peroxide ions, whereas at the exponent $n \approx 0.25$ for BSCFW2, the dominant species are ionized adatoms. This is apparently due to the defective surface structure of these oxides, which determines the difference in the rates of the stages observed in the equilibrium tracer oxygen exchange experiment for the BSCF and BSCFTa15 oxides. The stages of dissociative adsorption and oxygen incorporation for these oxides are competing. At the same time, for the BSCFW2 oxide, the rate-limiting stage is dissociative adsorption [17], and the dominant species on the surface are dissociated adatoms.

In order to analyze the differences between the absolute values of the chemical oxygen exchange coefficients k^δ, let us compare the tracer (k^*) and chemical (k^δ) exchange coefficients for the BSCF, BSCFTa15, and BSCFW2 oxides (Fig. 4).

Figure 4 shows that the oxides under study are divided into two groups: for the BSCF and BSCFTa15 oxides, the difference between k^δ and k^* is more than three orders of magnitude, while for BSCFW2 this difference is significantly smaller. As we previously noted in [17], the kinetics of oxygen exchange with the BSCF and BSCFTa15 oxides studied by equilibrium and nonequilibrium methods differs from that with BSCFW2, namely, in the rate of the stages and the degree of surface coverage by ionized oxygen species participating in the stage that determines the rate of oxygen exchange. In addition, it was shown in [38] that the atomicity of the oxygen particle participating in the stage that determines the rate of oxygen exchange with BSCFW2 differs from that for BSCF and BSCFTa15.

Table presents the surface thermodynamic factor $w_0|_{x=\pm L}$ calculated using Eq. (3) and the bulk thermodynamic factor w_0 calculated using Eq. (5) from the linear region of the dependence of oxygen content in the oxide on the temperature and partial pressure of oxygen.

Table shows that the bulk thermodynamic factors for all oxides have similar values of the order of a hundred and do not exceed $1.4 \cdot 10^2$, which may indicate a similarity in the mechanism of point defect formation. An increase in temperature and concentration of the alloying element leads to a decrease in the bulk thermodynamic factor $w_0|_{x=0}$ in the order from BSCF to BSCFW2 to BSCFTa15. This trend is consistent with the observed dependence of the Gibbs free energy of oxygen vacancy formation in these oxides on the oxygen content. Thus, the Gibbs free energy of oxygen formation increases in the order from BSCF to BSCFW2 to BSCFTa15 at the same concentration of oxygen vacancies [17]. In other words, the higher the concentration of the alloying element, the higher the energy required to form oxygen

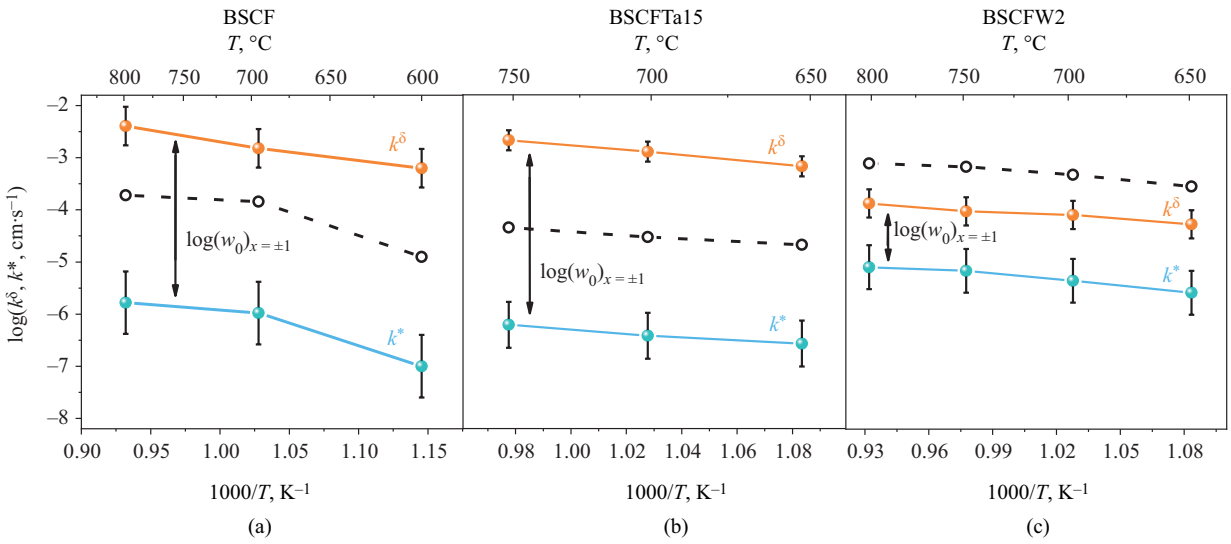

Fig. 4. Comparison of the tracer and chemical oxygen exchange coefficients for (a) BSCF, (b) BSCFTa15, and (c) BSCFW2 at an oxygen pressure of 6.7 mbar. The open circles connected by dashed lines represent the chemical oxygen exchange coefficients $k^{\delta'}$ calculated from the bulk thermodynamic coefficient $w_0|_{x=0}$ under the assumption $w_0|_{x=0} = w_0|_{x=\pm L}$ [38]

Table. Calculated values of the bulk $(w_0|_{x=0})$ and surface $(w_0|_{x=\pm L})$ thermodynamic factors

Oxide	T, °C	Thermodynamic factor	
		Surface $w_0\|_{x=\pm L}$	Bulk $w_0\|_{x=0}$
BSCF	600	$(6.3 \pm 0.9) \cdot 10^3$	$(1.3 \pm 0.1) \cdot 10^2$ [26]
	700	$(1.5 \pm 0.4) \cdot 10^3$	$(1.4 \pm 0.1) \cdot 10^2$ [26]
	800	$(2.4 \pm 0.6) \cdot 10^3$	$(1.2 \pm 0.1) \cdot 10^2$ [26]
BSCFTa15	650	$(2.5 \pm 0.7) \cdot 10^3$	$(0.8 \pm 0.1) \cdot 10^2$
	700	$(3.4 \pm 0.8) \cdot 10^3$	$(0.8 \pm 0.1) \cdot 10^2$
	750	$(3.5 \pm 0.8) \cdot 10^3$	$(0.7 \pm 0.1) \cdot 10^2$
BSCFW2	650	$(2.0 \pm 0.5) \cdot 10^1$	$(1.1 \pm 0.1) \cdot 10^2$
	700	$(1.8 \pm 0.5) \cdot 10^1$	$(1.1 \pm 0.1) \cdot 10^2$
	750	$(1.3 \pm 0.5) \cdot 10^1$	$(1.0 \pm 0.1) \cdot 10^2$
	800	$(1.6 \pm 0.5) \cdot 10^1$	$(0.9 \pm 0.1) \cdot 10^2$

vacancies. This is confirmed by the fact that oxygen content increases in the same series of oxides [17]. Thus, the bulk thermodynamic factor is directly determined by oxygen deficiency in the oxide.

A different picture is observed for the surface thermodynamic factor $w_0|_{x=\pm L}$. Higher values of $(1.5–6.3) \cdot 10^3$ are characteristic of the BSCF and BSCFTa15 oxides, while the values for BSCFW2 do not exceed 20. This discrepancy is unlikely to be related to the nature and concentration of the highly charged dopant. Apparently, these differences should be interpreted through a significant difference in the defective surface structure in the series of isomorphic oxides. This is confirmed by the results we obtained

by X-ray photoelectron spectroscopy of the surface of these oxides [17]. Thus, the surface layer at a depth of 5–10 nm for the BSCF and BSCFTa15 oxides consists of a Ba- and Co-containing phase with an undefined stoichiometry, and the surface layer at a depth of 1–5 nm comprises exclusively $BaCO_3$. Conversely, the surface of BSCFW2 is completely covered with $BaCO_3$.

Therefore, the observed difference in the values of surface thermodynamic factors for the BSCF, BSCFTa15, and BSCFW2 oxides clearly correlates with the difference in the slope of the dependence of k^δ on p_{O_2}. This observation reflects the difference in the mechanism of surface oxygen exchange. Specifically, for the BSCF and BSCFTa15 oxides, for which the dissociative oxygen adsorption stage and the oxygen incorporation stage compete and the dependence of the surface coverage with peroxide ions $O^{2-}_{2,ad}$ on p_{O_2} is proportional to the oxygen exchange rate under nonequilibrium conditions, high values of the surface thermodynamic factor exceed the bulk thermodynamic factor by 1.5−2.0 orders of magnitude. On the other hand, for the BSCFW2 oxide, for which the dissociative oxygen adsorption is the rate-limiting stage and the dependence of the surface coverage with single charged adatoms O^-_{ad} on p_{O_2} is proportional to the surface oxygen exchange rate, the values of the surface thermodynamic factor are 0.5−1.0 times the bulk thermodynamic factor, being significantly smaller than the surface factor for the BSCF and BSCFTa15 oxides. However, this does not allow a conclusion about the generality of the observed correlations for oxides with mixed conduction to be drawn. Literature data on k^δ and k^* for different oxide compositions can hardly be compared, since they were obtained under widely varying conditions for different oxides with different histories (e.g., synthesis method, experimental conditions, etc.). Further research is needed to identify general patterns concerning the oxygen exchange mechanism under equilibrium and nonequilibrium conditions.

The relationship between the thermodynamic factor and kinetic parameters was noted previously [33, 40–42]. It should be emphasized that the thermodynamic factor reflects the activity of an oxide system in response to changes in oxygen pressure and, thus, is directly related to the concentration of oxygen vacancies in the bulk or surface layers of the oxide material. In general, it is quite obvious that the structure of defects, which determines the oxygen exchange mechanism (including the concentration of point defects), differs significantly in the surface layers and in the bulk of the material. This was confirmed in numerous studies [17–19, 34–36, 43]. Given this "inequality" in the structure and composition of the bulk and surface, it becomes clear that the generally accepted [1, 20, 26, 30, 44–50] relationship between the tracer oxygen exchange coefficient k^* and the chemical oxygen exchange coefficient k^δ via the bulk thermodynamic factor $w_0|_{x=0}$ is inaccurate. A more accurate approach would be to introduce the surface thermodynamic factor $w_0|_{x=\pm L}$, which is described by Eq. (3).

It can be concluded that when selecting an oxide material for high-temperature electrochemical devices operating under a gradient of the electrochemical potential of oxygen, it is recommended to use oxides with the highest values of surface thermodynamic factors, represented by the difference between the surface tracer oxygen exchange coefficients and the chemical exchange coefficients, measured under the same experimental conditions.

CONCLUSIONS

The surface thermodynamic factor $w_0|_{x=\pm L}$ was calculated from the ratio of the chemical (k^δ) to the tracer (k^*) oxygen exchange coefficients for the BSCF, BSCFTa15, and BSCFW2 oxides. For the BSCF and BSCFTa15 oxides, the values of the surface factor exceed those of the bulk factor by 1.5–2.0 orders of magnitude. Conversely, for the BSCFW2 oxide, the surface thermodynamic factor was found to be 0.5–1.0 times the bulk thermodynamic factor. This difference was explained by differences in the defect structure of the oxide surfaces.

For identifying a more active material under electrochemical potential gradient conditions, we proposed a criterion represented by the ratio between the chemical and tracer oxygen exchange coefficients.

Acknowledgments

This work utilized the capabilities of the "Composition of Compounds" Shared Access Centers and the Unique "Isotope Exchange" Research Facility at the Institute of High-Temperature Electrochemistry, Ural Branch, Russian Academy of Sciences. This work was partially supported by the "Priority-2030" Development Program of the D.I. Mendeleev University of Chemical Technology of Russia. We also acknowledge the support of the EOTP-VE-665 project.

Authors' contributions

A.R. Akhmadeev—writing the text of the article, conducting experiments.

V.A. Eremin—conducting experiments.

M.V. Ananyev—conceptualization, editing the text of the article.

Conflicts of interest

The authors declare that they have no known competing financial interests or personal relationships that could have appeared to influence the work reported in this paper.

REFERENCES

1. Geffroy P.M., Fouletier J., Richet N., Chartier T. Rational selection of MIEC materials in energy production processes. *Chem. Eng. Sci.* 2013;87:408–433. https://doi.org/10.1016/j.ces.2012.10.027
2. Sunarso J., Baumann S., Serra J.M., Meulenberg W.A., Liu S., Lin Y.S., Diniz da Costa J.C. Mixed ionic-electronic conducting (MIEC) ceramic-based membranes for oxygen separation. *J. Membrane Sci.* 2008;320(1-2):13–41. https://doi.org/10.1016/j.memsci.2008.03.074
3. Sahini M.G., Mwankemwa B.S., Kanas N. $Ba_xSr_{1-x}Co_yFe_{1-y}O_{3-\delta}$ (BSCF) mixed ionic-electronic conducting (MIEC) materials for oxygen separation membrane and SOFC applications: Insights into processing, stability, and functional properties. *Ceramics Int.* 2022;48(3):2948–2964. https://doi.org/10.1016/j.ceramint.2021.10.189
4. Bouwmeester H.J.M., Burggraaf A.J. Chapter 10. Dense ceramic membranes for oxygen separation. In: *Membrane Science and Technology*. V. 4. Elsevier; 1996. P. 435–528. https://doi.org/10.1016/S0927-5193(96)80013-1
5. Markov A.A., Merkulov O.V., Suntsov A.Yu. Development of Membrane Reactor Coupling Hydrogen and Syngas Production. *Membranes.* 2023;13(7):626. https://doi.org/10.3390/membranes13070626
6. Sunarso J., Hashim S.S., Zhu N., Zhou W. Perovskite oxides applications in high temperature oxygen separation, solid oxide fuel cell and membrane reactor: A review. *Progress in Energy and Combustion Science*. 2017;61:57–77. https://doi.org/10.1016/j.pecs.2017.03.003
7. Suntsov A.Yu., Marshenya S.N., Markov A.A., Kozhevnikov V.L. Performance of the layered cobaltites in membrane mediated oxygen separation from air and methane partial oxidation. *Mater. Lett.* 2021;295:129818. https://doi.org/10.1016/j.matlet.2021.129818
8. Bouwmeester H.J.M., Kruidhof H., Burggraaf A.J. Importance of the surface exchange kinetics as rate limiting step in oxygen permeation through mixed-conducting oxides. *Solid State Ionics.* 1994;72(Part 2):185–194. https://doi.org/10.1016/0167-2738(94)90145-7
9. Lin Y.-S., Wang W., Han J. Oxygen permeation through thin mixed-conducting solid oxide membranes. *AIChE J.* 1994;40:786–798. https://doi.org/10.1002/aic.690400506
10. Bouwmeester H.J.M., Krmdhof H., Burggraaf A.J., Gelhngs P.J. Oxygen semipermeability of erbia-stabilized bismuth oxide. *Solid State Ionics*. 1992;53-56(Part 1): 460–468. https://doi.org/10.1016/0167-2738(92)90416-M
11. Dou S., Masson C.R., Pacey P.D. Mechanism of Oxygen Permeation Through Lime-Stabilized Zirconia. *J. Electrochem. Soc*. 1985;132(8):1843–1849. https://doi.org/10.1149/1.2114228
12. Vanhassel B., Kawada T., Sakai N., Yokokawa H., Dokiya M., Bouwmeester H. Oxygen permeation modelling of perovskites. *Solid State Ionics*. 1993;66(3-4):295–305. https://doi.org/10.1016/0167-2738(93)90419-4
13. Cao G.Z. Electrical conductivity and oxygen semipermeability of terbia and yttria stabilized zirconia. *J. Appl. Electrochem*. 1994;24:1222–1227. https://doi.org/10.1007/BF00249885
14. Wagner C. Beitrag zur Theorie des Anlaufvorgangs. *Z. Physikal. Chem*. 1933;21B(1):25–41. https://doi.org/10.1515/zpch-1933-2105
15. Wagner C. Beitrag zur Theorie des Anlaufvorganges. II. *Z. Physikal. Chem*. 1936;32B(1):447–462. https://doi.org/10.1515/zpch-1936-3239
16. Wagner C. Equations for transport in solid oxides and sulfides of transition metals. *Progress in Solid State Chemistry*. 1975;10(Part 1): 3–16. https://doi.org/10.1016/0079-6786(75)90002-3
17. Akhmadeev A.R., Eremin V.A., Ananyev M.V., Voloshin B.V., Popov M.P., Ivanov I.L., Fetisov A.V. Oxygen stoichiometry and isotope exchange of oxides $Ba_{0.5}Sr_{0.5}Co_{0.8}Fe_{0.2}O_{3-\delta}$ doped with Ta, Nb, Mo or W. *Appl. Surface Sci.* 2023;629:157312. https://doi.org/10.1016/j.apsusc.2023.157312
18. Eremin V.A., Ananyev M.V., Bouwmeester H.J.M., Kurumchin E.K., Yoo C.Y. Oxygen surface exchange kinetics of $Ba_{0.5}Sr_{0.5}Co_{0.8}Fe_{0.2}O_{3-\delta}$. *Phys. Chem. Chem. Phys*. 2020;22(18):10158–10169. https://doi.org/10.1039/c9cp06650k
19. Ananyev M.V., Eremin V.A., Tsvetkov D.S., Porotnikova N.M., Farlenkov A.S., Zuev A.Y., Fetisov A.V., Kurumchin E.K. Oxygen isotope exchange and diffusion in $LnBaCo_2O_{6-\delta}$ (Ln = Pr, Sm, Gd) with double perovskite structure. *Solid State Ionics*. 2017;304: 96–106. https://doi.org/10.1016/j.ssi.2017.03.022
20. Berenov A.V., Atkinson A., Kilner J.A., Bucher E., Sitte W. Oxygen tracer diffusion and surface exchange kinetics in $La_{0.6}Sr_{0.4}CoO_{3-\delta}$. *Solid State Ionics*. 2010;181(17-18): 819–826. https://doi.org/10.1016/j.ssi.2010.04.031
21. Benson S.J., Chater R., Kilner J.A. Oxygen diffusion and surface exchange in the mixed conducting perovskite $La_{0.6}Sr_{0.4}Fe_{0.8}Co_{0.2}O_{3-\delta}$. In: Ramanarayanan T.A. (Ed.). *Ionic and Mixed Conducting Ceramics: Proceedings of the Third International Symposium*. Electrochemical Society; 1998. V. 97–24. P. 596–609. https://books.google.ru/books?id=30NC4dcoghAC&hl=ru&source=gbs_navlinks_s
22. Wang L., Merkle R., Maier J., Acartürk T., Starke U. Oxygen tracer diffusion in dense $Ba_{0.5}Sr_{0.5}Co_{0.8}Fe_{0.2}O_{3-\delta}$ films. *Appl. Phys. Lett*. 2009;94:071908. https://doi.org/10.1063/1.3085969
23. Fullarton I.C., Jacobs J.-P., Van Benthem H.E., Kilner J.A., Brongersma H.H., Scanlon P.J., Steele B.C.H. Study of oxygen ion transport in acceptor doped samarium cobalt oxide. *Ionics.* 1995;1:51–58. https://doi.org/10.1007/BF02426008
24. De Souza R.A., Kilner J.A. Oxygen transport in $La_{1-x}Sr_xMn_{1-y}Co_yO_{3\pm\delta}$ perovskites: Part I. Oxygen tracer diffusion. *Solid State Ionics*. 1998;106(3-4):175–187. https://doi.org/10.1016/s0167-2738(97)00499-2
25. Kriegel R., Kircheisen R., Töpfer J. Oxygen stoichiometry and expansion behavior of $Ba_{0.5}Sr_{0.5}Co_{0.8}Fe_{0.2}O_{3-\delta}$. *Solid State Ionics.* 2010;181(1-2):64–70. https://doi.org/10.1016/j.ssi.2009.11.012
26. Bucher E., Egger A., Ried P., Sitte W., Holtappels P. Oxygen nonstoichiometry and exchange kinetics of $Ba_{0.5}Sr_{0.5}Co_{0.8}Fe_{0.2}O_{3-\delta}$. *Solid State Ionics.* 2008;179(21-26): 1032–1035. https://doi.org/10.1016/j.ssi.2008.01.089
27. McIntosh S., Vente J.F., Haije W.G., Blank D.H.A., Bouwmeester H.J.M. Structure and oxygen stoichiometry of $SrCo_{0.8}Fe_{0.2}O_{3-\delta}$ and $Ba_{0.5}Sr_{0.5}Co_{0.8}Fe_{0.2}O_{3-\delta}$. *Solid State Ionics*. 2006;177(19-25):1737–1742. https://doi.org/10.1016/j.ssi.2006.03.041
28. Jun A., Yoo S., Gwon O.H., Shin J., Kim G. Thermodynamic and electrical properties of $Ba_{0.5}Sr_{0.5}Co_{0.8}Fe_{0.2}O_{3-\delta}$ and $La_{0.6}Sr_{0.4}Co_{0.2}Fe_{0.8}O_{3-\delta}$ for intermediate-temperature solid oxide fuel cells. *Electrochimica Acta*. 2013;89:372–376. https://doi.org/10.1016/j.electacta.2012.11.002
29. Mueller D.N., De Souza R.A., Yoo H.I., Martin M. Phase stability and oxygen nonstoichiometry of highly oxygen-deficient perovskite-type oxides: A case study of $(Ba,Sr)(Co,Fe)O_{3-\delta}$. *Chem. Mater*. 2012;24(2):269–274. https://doi.org/10.1021/cm2033004

30. Wang L., Merkle R., Mastrikov Y.A., Kotomin E.A., Maier J. Oxygen exchange kinetics on solid oxide fuel cell cathode materials-general trends and their mechanistic interpretation. *J. Mater. Res*. 2012;27(15):2000–2008. https://doi.org/10.1557/jmr.2012.186
31. Bouwmeester H.J.M., Song C., Zhu J., Yi J., Van Sint Annaland M., Boukamp B.A. A novel pulse isotopic exchange technique for rapid determination of the oxygen surface exchange rate of oxide ion conductors. *Phys. Chem. Chem. Phys.* 2009;11(42): 9640–9643. https://doi.org/10.1039/b912712g
32. Berenov A., Atkinson A., Kilner J., Ananyev M., Eremin V., Porotnikova N., Farlenkov A., Kurumchin E., Bouwmeester H.J.M., Bucher E., Sitte W. Oxygen tracer diffusion and surface exchange kinetics in $Ba_{0.5}Sr_{0.5}Co_{0.8}Fe_{0.2}O_{3-\delta}$. *Solid State Ionics*. 20914;268(Part A): 102–109. https://doi.org/10.1016/j.ssi.2014.09.031
33. Maier J. On the correlation of macroscopic and microscopic rate constants in solid state chemistry. *Solid State Ionics.* 1998; 112(3-4):197–228. https://doi.org/10.1016/S0167-2738(98)00152-0
34. Ananyev M.V., Porotnikova N.M., Kurumchin E.K. Influence of strontium content on the oxygen surface exchange kinetics and oxygen diffusion in $La_{1-x}Sr_xCoO_{3-\delta}$ oxides. *Solid State Ionics*. 2019;341:115052. https://doi.org/10.1016/j.ssi.2019.115052
35. Ananyev M.V., Tropin E.S., Eremin V.A., Farlenkov A.S., Smirnov A.S., Kolchugin A.A., Porotnikova N.M., Khodimchuk A.V., Berenov A.V., Kurumchin E.Kh. Oxygen isotope exchange in $La_2NiO_{4\pm\delta}$. *Phys. Chem. Chem. Phys.* 2016;18(13):9102–9111. https://doi.org/10.1039/C5CP05984D
36. Porotnikova N.M., Eremin V.A., Farlenkov A.S., Kurumchin E.K., Sherstobitova E.A., Kochubey D.I., Ananyev M.V. Effect of AO Segregation on Catalytical Activity of $La_{0.7}A_{0.3}MnO_{3\pm\delta}$ (A = Ca, Sr, Ba) Regarding Oxygen Reduction Reaction. *Catal. Lett.* 2018;148: 2839–2847. https://doi.org/10.1007/s10562-018-2456-7
37. Popov M.P., Starkov I.A., Bychkov S.F., Nemudry A.P. Improvement of $Ba_{0.5}Sr_{0.5}Co_{0.8}Fe_{0.2}O_{3-\delta}$ functional properties by partial substitution of cobalt with tungsten. *J. Membrane Sci.* 2014;469:88–94. https://doi.org/10.1016/j.memsci.2014.06.022
38. Akhmadeev A.R., Eremin V.A., Ananyev M.V. Kinetics of oxygen exchange with oxides $Ba_{0.5}Sr_{0.5}(Co_{0.8}Fe_{0.2})_{1-x}Me_xO_{3-\delta}$ (Me = Ta, W) in non-equilibrium conditions. *J. Solid State Electrochem*. 2024;29:4973–4983. https://doi.org/10.1007/s10008-024-06034-x
39. Fleig J., Merkle R., Maier J. The $p(O_2)$ dependence of oxygen surface coverage and exchange current density of mixed conducting oxide electrodes: model considerations. *Phys. Chem. Chem. Phys.* 2007;9(21):2713–2723. https://doi.org/10.1039/b618765j
40. Maier J. Interaction of oxygen with oxides: How to interpret measured effective rate constants? *Solid State Ionics*. 2000; 135(1-4):575–588. https://doi.org/10.1016/S0167-2738(00)00438-0
41. Adler S., Chen X., Wilson J. Mechanisms and rate laws for oxygen exchange on mixed-conducting oxide surfaces. *J. Catalysis*. 2007;245(1):91–109. https://doi.org/10.1016/j.jcat.2006.09.019
42. Adler S.B. Factors governing oxygen reduction in solid oxide fuel cell cathodes. *Chem. Rev*. 2004;104(10):4791–4843. https://doi.org/10.1021/cr020724o
43. Porotnikova N., Farlenkov A., Naumov S., Vlasov M., Khodimchuk A., Fetisov A., Ananyev M. Effect of grain boundaries in $La_{0.8}4Sr_{0.16}CoO_{3-\delta}$ on oxygen diffusivity and surface exchange kinetics. *Phys. Chem. Chem. Phys*. 2021;23(19):11272–11286. https://doi.org/10.1039/d1cp01099a
44. Ten Elshof J.E., Lankhorst M.H.R., Bouwmeester H.J.M. Oxygen Exchange and Diffusion Coefficients of Strontium-Doped Lanthanum Ferrites by Electrical Conductivity Relaxation. *J. Electrochem. Soc.* 1997;144(3):1060–1067. https://doi.org/10.1149/1.1837531
45. Lane J.A., Benson S.J., Waller D., Kilner J.A. Oxygen transport in $La_{0.6}Sr_{0.4}Co_{0.2}Fe_{0.8}O_{3-\delta}$. *Solid State Ionics*. 1999;121(1-4): 201–208. https://doi.org/10.1016/S0167-2738(99)00014-4
46. Geffroy P.M., Blond E., Richet N., Chartier T. Understanding and identifying the oxygen transport mechanisms through a mixed-conductor membrane. *Chem. Eng. Sci*. 2017;162: 245–261. https://doi.org/10.1016/j.ces.2017.01.006
47. Egger A., Bucher E., Yang M., Sitte W. Comparison of oxygen exchange kinetics of the IT-SOFC cathode materials $La_{0.5}Sr_{0.5}CoO_{3-\delta}$ and $La_{0.6}Sr_{0.4}CoO_{3-\delta}$. *Solid State Ionics*. 2012;225:55–60. https://doi.org/10.1016/j.ssi.2012.02.050
48. Ten Elshof J.E., Lankhorst M.H.R., Bouwmeester H.J.M. Chemical diffusion and oxygen exchange of $La_{0.6}Sr_{0.4}Co_{0.6}Fe_{0.4}O_{3-\delta}$. *Solid State Ionics*. 1997;99(1-2):15–22. https://doi.org/10.1016/S0167-2738(97)00263-4
49. Katsuki M. High temperature properties of $La_{0.6}Sr_{0.4}Co_{0.8}Fe_{0.2}O_{3-\delta}$ oxygen nonstoichiometry and chemical diffusion constant. *Solid State Ionics*. 2003;156(3-4): 453–461. https://doi.org/10.1016/S0167-2738(02)00733-6
50. Gao Z., Mogni L.V., Miller E.C., Railsback J.G., Barnett S.A. A perspective on low-temperature solid oxide fuel cells. *Energy Environ. Sci*. 2016;9(5):1602–1644. https://doi.org/10.1039/C5EE03858H

About the Authors

Albert R. Akhmadeev, Postgraduate Student, Federal Research Center of Problems of Chemical Physics and Medical Chemistry, Russian Academy of Sciences (1, Severnyi pr., Chernogolovka, Moscow oblast, 142432, Russia); Senior Researcher, Laboratory of the Electrochemical Devices for Hydrogen Energy, Giredmet JSC (2-1, Electrodnaya ul., Moscow, 111524, Russia). E-mail: albertakhmadeev1@gmail.com. ResearcherID HPF-3683-2023, Scopus Author ID 58243031000, RSCI SPIN-code 2550-5154, https://orcid.org/0000-0003-3863-0043

Vadim A. Eremin, Cand. Sci. (Chem.), Head of the Laboratory of the Electrochemical Devices for Hydrogen Energy, Giredmet JSC (2-1, Electrodnaya ul., Moscow, 111524, Russia). E-mail: v-eremin@list.ru. Scopus Author ID 7103377859, ResearcherID L-6709-2017, RSCI SPIN-code 4346-9175, https://orcid.org/0000-0002-1897-4618

Maxim V. Ananyev, Dr. Sci. (Chem.), Head of the Department of the Technology and Materials of the Fourth Energy, Giredmet JSC (2-1, Electrodnaya ul., Moscow, 111524, Russia); Professor, Department of Information Computer Technologies, Mendeleev University of Chemical Technology of Russia (9, Miusskaya pl., Moscow, 125047, Russia). E-mail: m.ananyev@mail.ru. Scopus Author ID 15061114600, ResearcherID F-5104-2014, RSCI SPIN-code 7820-0441, https://orcid.org/0000-0002-2254-0193

Об авторах

Ахмадеев Альберт Рустемович, аспирант, ФГБУН Федеральный исследовательский центр проблем химической физики и медицинской химии Российской академии наук (ФИЦ ПХФ и МХ РАН) (142432, Россия, Московская обл., г. Черноголовка, Северный пр., д. 1); старший научный сотрудник лаборатории Электрохимических устройств для водородной энергетики, АО «Государственный научно-исследовательский и проектный институт редкометаллической промышленности «Гиредмет» имени Н.П. Сажина (111524, Россия, Москва, Электродная ул., д. 2, стр. 1). E-mail: albertakhmadeev1@gmail.com. Scopus Author ID 58243031000, ResearcherID HPF-3683-2023, SPIN-код РИНЦ 2550-5154, https://orcid.org/0000-0003-3863-0043

Еремин Вадим Анатольевич, к.х.н., начальник лаборатории Электрохимических устройств для водородной энергетики, АО «Государственный научно-исследовательский и проектный институт редкометаллической промышленности «Гиредмет» имени Н.П. Сажина (111524, Россия, Москва, Электродная ул., д. 2, стр. 1). E-mail: v-eremin@list.ru. Scopus Author ID 7103377859, ResearcherID L-6709-2017, SPIN-код РИНЦ 4346-9175, https://orcid.org/0000-0002-1897-4618

Ананьев Максим Васильевич, д.х.н., начальник Управления технологий и Материалов Четвертого Энергетического Перехода, АО «Государственный научно-исследовательский и проектный институт редкометаллической промышленности «Гиредмет» имени Н.П. Сажина (111524, Россия, Москва, Электродная ул., д. 2, стр. 1); профессор кафедры информационных компьютерных технологий, ФГБОУ ВО «Российский химико-технологический университет имени Д.И. Менделеева» (125047, Россия, Москва, Миусская пл., д. 9). E-mail: m.ananyev@mail.ru. Scopus Author ID 15061114600, ResearcherID F-5104-2014, SPIN-код РИНЦ 7820-0441, https://orcid.org/0000-0002-2254-0193

Translated from Russian into English by V. Glyanchenko
Edited for English language and spelling by Dr. David Mossop